Neodymium ions activated barium ferrite composites for microwave X-band absorber applications: synthesis and characterizations

by Wahyu Widanarto

Submission date: 04-Mar-2020 08:49PM (UTC+0700)
Submission ID: 1269110637
File name: Manuscript_NdBFC_20200217-c-revisi.docx (325.91K)
Word count: 3628
Character count: 20883

Neodymium ions activated barium ferrite composites for microwave X-band absorber applications: synthesis and characterizations

Wahyu Widanarto [a,*], Ananda Iqbal Ekaputra [a], Mukhtar Effendi [a], Wahyu Tri Cahyanto [a], Sib Krishna Ghoshal [b], Candra Kurniawan [c], Erfan Handoko [d], Mudrik Alaydrus [e]

[a] Department of Physics, FMIPA, Universitas Jenderal Soedirman, Jl. dr. Soeparno 61 Purwokerto 53123, Indonesia
[b] Department of Physics and Laser Centre, AMORG, Faculty of Science, Universiti Teknologi Malaysia, Johor Bahru, Skudai 81310, Malaysia
[c] Research Center for Physics, Indonesian Institute of Sciences (LIPI), Puspiptek Office Area, South Tangerang, Banten 15314, Indonesia
[d] Department of Physics, Universitas Negeri Jakarta, Jl. Rawamangun Muka, Jakarta 13220, Indonesia
[e] Department of Electrical Engineering, Universitas Mercu Buana, Jl. Meruya Selatan, Jakarta 11650, Indonesia
* Corresponding Author: Tel.: +62 85726996007
E-mail address: wahyu.widanarto@unsoed.ac.id (W. Widanarto)

ABSTRACT

Some composites of barium ferrites activated with the neodymium ions (Nd^{3+}) of composition (20)BaO:(80-x)γ-Fe_2O_3:(x)Nd_2O_3 (x = 0, 1, and 2 mol%) were synthesized using the modified mechanical alloying for the first time. The influence of varying Nd^{3+} concentrations on the morphologies, microstructures, and magnetic characteristics of these composites were evaluated. In addition, the microwave (MW) reflection loss, complex relative permittivity, and permeability of the studied composites in the frequency range of 8.2 – 12.4 GHz were analysed using the Nicholson-Ross-Weir (NRW) method. The inclusion of Nd^{3+} in the proposed composites was discerned to influence the permittivity, permeability and reflection loss significantly in the MW X-band region.

Keywords: neodymium, magnetic properties, permittivity, permeability, reflection loss

1. Introduction

Recent studies revealed that the inclusion (as dopant) of various divalent or trivalent rare-earth ions (REIs) into the crystal structure of the barium hexaferrites (BHFs) can change their magnetic properties (such as coercivity (H_c), remanent magnetization (M_r) and saturation magnetization (M_s), natural resonant frequency, complex relative permeability ($\mu' + i\mu''$) and permittivity ($\varepsilon' + i\varepsilon''$) as well as the magnetic field anisotropy [1,2]. Consequently, the influence of electromagnetic interference on such ferrites can be strengthened. Additionally, the excellent compatibility related to the hexagonal lattice structure and extraordinary relaxational attributes of the REIs (act as dopant or activator also called surrogate ions) has also been exploited over the decades by activating them inside various crystals, glasses, and glass-ceramics. It has been established that by doping these REIs inside the BHFs their magnetic and MW absorption properties can remarkably be altered and customized [3–7]. In addition, the REIs-doped BHFs that possess weak H_c and low M_s are beneficial for enhancing the MW absorption capacity [8–11]. Based on these factors, we prepared some barium ferrite composites (BFCs) doped with Nd^{3+} to determine the feasibility of enhancing the MW X-band absorption frequency by reducing the values of H_c and M_s.

Of late, several physical and chemical techniques have been developed to synthesize submicron particles of BHFs such as the solid-state reaction, mechanical alloying, co-precipitation, electrostatic self-assembly, sol-gel process, and combustion methods [12–19]. These methods play a significant role in controlling the morphologies (sizes and shapes), structures, and magnetic characteristics of the produced BHFs. In addition, dedicated efforts have been made to modify the structures, morphologies and magnetic properties of various functional materials to obtain the best MW absorbing attributes [19–22]. Amongst these synthesis techniques, the mechanical alloying being a low-cost and simple approach can produce BHF powder with distinct attributes such as the wide specific area of the grain boundary and high atomic volume fraction at the boundary [8]. Despite some efforts, an accurate method to synthesize the Nd^{3+}-doped BHF composites with controlled magnetic and MW absorption characteristics has been deficient.

Considering the diverse applied interests of REIs-doped BHFs we prepared some new types of Nd^{3+}-doped BF composites (hereinafter named as NdBFCs) using the modified mechanical alloying and characterized them. The role of different Nd^{3+} doping levels on the structural, morphological, magnetic and MW absorption traits of these NdBFC was determined. Besides, the MW reflection loss (R_L) of the proposed NdBFCs in the frequency (f) range of 8.2-12.4 GHz was evaluated to determine their feasibility in favor of MW X-band absorber applications.

2. Material and Methods

Three NdBFCs of chemical composition (20)BaO:(80-x)γ-Fe_2O_3:(x)Nd_2O_3, where x = 0, 1 and 2 mol% were prepared by the mechanical alloying strategy. Analytical grade chemical reagents (all in powder form) of barium carbonate [$BaCO_3$, Merck purity of 99%], neodymium oxide [Nd_2O_3, Sigma Aldrich of purity 99%] and natural gamma phase iron oxide [γ-Fe_2O_3, Sigma Aldrich of purity 99%] were utilized as the starting raw materials to prepare the proposed composites. Firstly, the milled iron sand was calcinated in an air atmosphere at 850 °C for 3 hours to acquire the natural γ-Fe_2O_3. Meanwhile, the $BaCO_3$ powder was calcinated in an air atmosphere at 350 °C for an hour to achieve the BaO powder by removing the existing carbon component. Then, the constituent materials with the nominal compositions were placed into a vial before being blended and milled using a Shaker Mill PPF-UG system for three hours in the on (5 min) and off (10 min) modes to achieve the homogeneous mixture of composite powders. Later, the fine powders were compacted to get pellets of 1 mm thick and 10 mm diameter [9]. The obtained pellets were strengthened using an electrical tube furnace (operated at 800 °C for an hour) and then sintered at 1100 °C for 5 hours with the heating rate of 10 °C/min in an air atmosphere before being cooled down normally to the ambient temperature. Depending on the Nd^{3+} doing contents

of 0, 1, and 2 mol% these pellets were coded as NdBFC0, NdBFC1, and NdBFC2. For the additional analyses, some of the pellets were crushed and bound using the epoxy resin to impart a rectangular shape consistent with the WR90 sample holder (dimension of 2.3 cm × 1.0 cm × 0.5 cm).

The morphology and microstructural analyses of the as-prepared NdBFCs were performed using the Hitachi (SU 3500) scanning electron microscopy (SEM) [9,11,23]. The crystal structures and phases of the NdBFCs were recorded on a SmartLab (3 kW) X-ray diffractometer equipped with Cu–Kα line of λ ≈ 0.1541874 nm. An Oxford (1.2H) vibrating sample magnetometer (VSM) was used to measure the magnetic properties of the NdBFCs. A Keysight (PNA-L N5232A) vector network analyzer (VNA) was used (in the range of 8–13 GHz) to measure the scattering parameters (S) of the prepared NdBFCs. The MW absorption measurement was carried out to yield the components of S (values of S_{11}, S_{12}, S_{21}, and S_{22}) wherein the values of S_{11} and S_{21} signified the coefficient of reflection (Γ) and transmission (T), respectively. The measured values of S_{22} and S_{12} were disregarded due to their equivalence to S_{11} and S_{21}, respectively. The Nicholson-Ross-Weir (NRW) method was followed to obtain the values of relative complex permeability (μ_r) and permittivity (ε_r).

3. Results and Discussion

Fig. 1 shows the SEM micrographs of the studied NdBFCs, which consisted of roughened porous microstructures. The substitution of Nd^{3+} into the crystal lattice of the NdBFCs was found to affect significantly the surface morphologies (grain sizes and shapes) and distributions of the grains. The average size of the NdBFC grains was decreased and the porosity was increased with the increase in the Nd^{3+} levels. It was argued that the enhanced porous structures are advantageous to achieve a longer propagation path for the electromagnetic waves, thereby effective for stronger reflections and scattering [24]. In addition, the magnetic characteristics and loss of MW reflection can be improved by increasing the porosity of the NdBFCs [11].

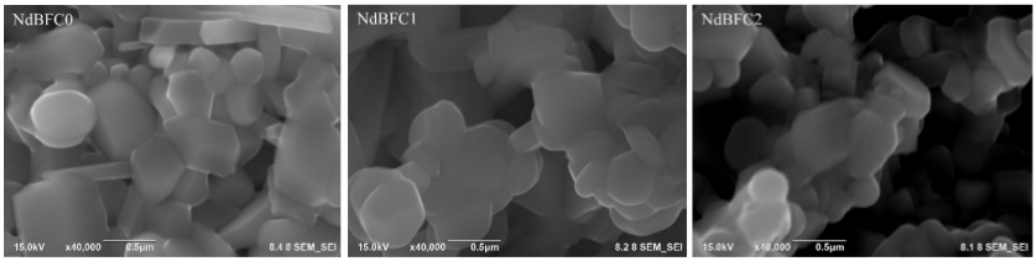

Fig. 1. The SEM images of the obtained NdBFCs

Fig. 2 shows the XRD pattern of the prepared NdBFCs, which comprised of several sharp peaks characteristics of different crystalline lattice planes. The observed peaks for the NdBFC0 sample (without Nd^{3+} doping) were allocated to the major hexagonal crystal structure of $BaFe_{12}O_{19}$ that matched to the ICDD number 00-039-1433 with lattice parameters $a = b = 0.5894$ nm, $c = 2.3215$ nm, $\alpha = \beta = 90°$ and $\gamma = 120°$. Conversely, the α-Fe_2O_3 rhombohedral crystal structure (ICDD number 00-033-0664) appeared at 33.336°. The crystal structure of the studied NdBFCs was significantly altered with the inclusion of Nd_2O_3 of 1 mol% as seen from the XRD pattern of NdBFC1. The appearance of six new peaks in the NdBFC1 sample was consistent with the orthorhombic crystal structure of $BaNd_2O_4$ (ICDD number 00-042-1499). Finally, the NdBFC2 sample containing Nd_2O_3 of 2 mol% disclosed a phase transformation from the hexagonal $BaFe_{12}O_{19}$ to hexagonal $Ba_3Fe_{32}O_{51}$ (ICDD number 00-041-0846). It was affirmed that substitution of Nd_2O_3 into the crystal structures of the BFC indeed produced a new primary hexagonal crystalline phase from $Ba_3Fe_{32}O_{51}$. The observed broadening in the diffraction peaks associated with all the prepared NdBFCs was due to the emergence of the quantum size effects (nanoscale particles) and lattice strain [25,26].

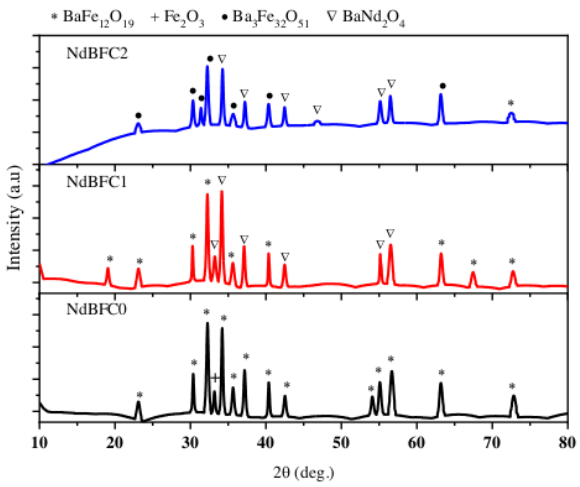

Fig. 2. The XRD patterns of the prepared NdBFCs.

Fig. 3 illustrates the magnetic field (H) dependent magnetization (M) response (hysteresis loop) of the NdBFCs. The values of M_s, M_r, and H_c for the pristine sample (NdBFC0) were 33.54 emu/g, 11.56 emu/g, and 726.06 Oe, respectively. The value M_s of the composites changes significantly because of the expansion concentration of Nd_2O_3. The value of M_s was lowered with the addition of 1 mol% of Nd_2O_3 into the composite (NdBFC1) which was possibly due to the

formation of anti-magnetic material ($BaNd_2O_4$). Furthermore, the value of M_s was increased due to the incorporation of 2 mol% of Nd_2O_3 into the composite (NdBFC2) and became higher than NdBFC0, which may be ascribed to the occurrence of a new phase of barium hexaferrite ($Ba_3Fe_{32}O_{51}$), increased porosity and higher surface roughness. It was argued that such enhanced porosity with extremely roughened granular surfaces might have alienated the magnetic domain walls, enabling regular polarizations of the unpaired spin magnetic moments when a magnetic field is applied externally.

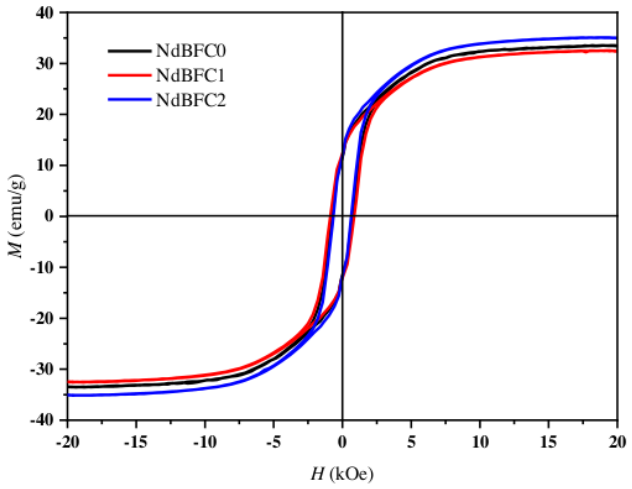

Fig. 3. The hysteresis loops of the as-prepared NdBFCs.

Fig. 4(a) depicts the frequency (ranged from 8.2–12.4 GHz) dependence of complex relative permeability (real, μ' and imaginary, μ'' parts) of the NdBFCs. The value μ' of all the NdBFCs was increased significantly in the lower MW frequency region and then decreased gradually in the higher frequency region. The onset of the decreasing permeability was approximately 8.5 GHz for the undoped sample (NdBFC0) and approximately 9.3 GHz for the doped composites (NdBFC and NdBFC2). The magnetic energy storing ability of the proposed NdBFCs was primarily ascribed to the natural spin magnetic moments' polarizations. Moreover, the value of μ'' (signifies the magnetic loss factor) was decreased rapidly to zero at approximately 8.5 GHz for the pristine sample and 9.3 GHz for the doped ferrites, confirming the absence of magnetic loss in the higher region. It is important to note that the imaginary permeability plays an essential role in the microwave absorption traits of hexaferrite [27] via the relaxation of the domain wall resonance [28].

Fig. 4(b) shows the frequency (ranged from 8.2–12.4 GHz) dependent complex relative permittivity (real, ε' and imaginary, ε'' components) of the NdBFCs. The intrinsic electric dipole polarizations in the MW frequency domain of the NdBFCs were responsible for the Type equation here.emergence of ε' and ε'' [29,30]. The real permittivity signified the energy stored in the material from an external electric field [31]. For the undoped or pristine sample (NdBFC0), the real permittivity was first increased up to 3 with the increase in the frequency and then decreased to nearly -1 above 12 GHz. Conversely, the real permittivity for the doped samples (NdBFC1 and NdBFC2) was first dropped in the low-frequency region and then increased up to 2 with the rise in the frequency. The ε'' of the undoped specimen (NdBFC0) revealed a shrinking tendency while for the doped samples (NdBFC1 and NdBFC2) it dropped rapidly below 8.2 GHz before being reached nearly to zero in the high-frequency region. The observed almost similar nature of the permittivity for both NdBFC1 and NdBFC2 is due to the presence of the non-magnetic phase of $BaNd_2O_4$ in the samples, resulting in the intrinsic electric dipole polarizations. However, the little difference in the permeability between NdBFC1 and NdBFC2 may be due to the existence of different amounts of the $BaFe_9O_{12}$ and $Ba_3Fe_{32}O_5$ phases with different magnetic properties. Thus, both phases played an important role in the permeability changes associated with the magnetic properties. In addition, a significant increase in the permittivity is possibly triggered by the dipolar polarization originated from the bond formation between O^{2-} with Ba^{2+} and Nd^{3+} in the non-magnetic $BaNd_2O_4$ phase.

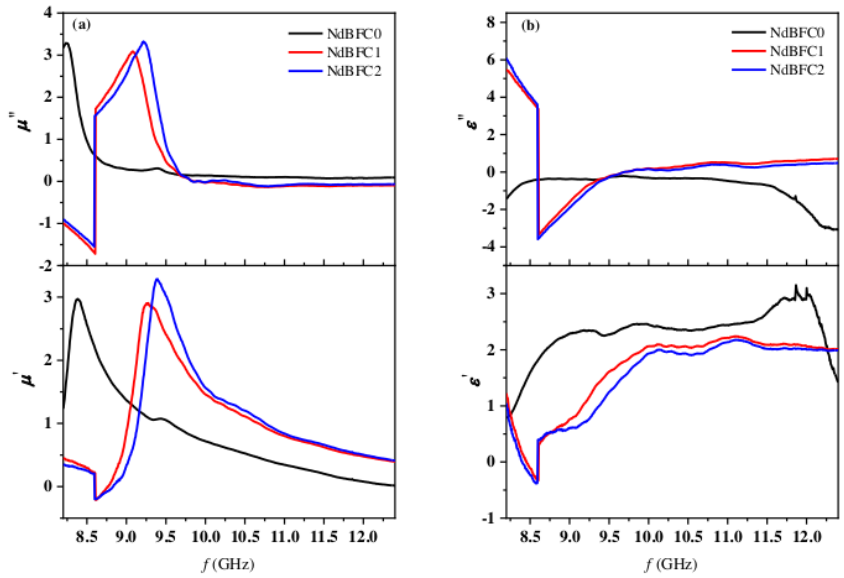

Fig. 4. Frequency-dependent (a) permeability and (b) permittivity of the NdBFCs with a thickness of 0.5 cm

Fig. 5 displays the f against R_L plot of the synthesized NdBFCs. The undoped specimen (NdBFC0) revealed three prominent absorption bands centered at approximately 8.4, 10, and 11 GHz with the corresponding R_L values of -37, -17, and -16 dB. Meanwhile, the graph for both the doped samples NdBFC1 and NdBFC2 showed a similar spectral pattern, which consisted of 4 durable absorption bands with values less than -10 dB accompanied by a significant shift. The observed shift in the peak frequency (toward the higher value) with the increase in the Nd^{3+} doping level was probably due to the enhanced porosity and emergence of a new barium hexaferrite phase ($Ba_3Fe_{32}O_{51}$) as well as $BaNd_2O_4$ in the composite structure. Consequently, the values of H_c, M_s, M_r, permeability, and permittivity of the prepared NdBFCs were modified. This, in turn, led to an alteration in the natural resonance frequency and impedance [32–34], thereby a shift in the *peak* R_L value towards higher frequency. It was also shown that the addition of Nd^{3+} caused a widening of the bandwidth in the 9-10 GHz frequency region and the R_L signals were more reversible to the MW frequencies compared to the previous findings [8,35,36].

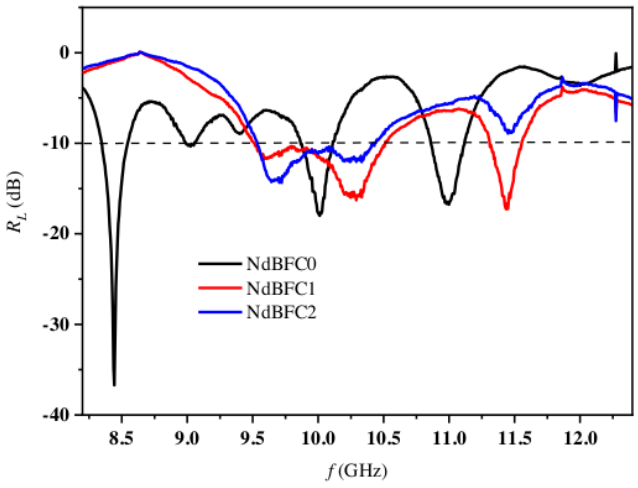

Fig. 5. The MW reflection loss as a function of the frequency for the studied NdBFCs of 0.5 cm thick

4. Conclusions

Following the modified mechanical alloying, a new type of Nd^{3+} activated BFCs was synthesized for the first time and characterized. The incorporation of Nd^{3+} into the hexagonal crystal lattice of BFs was found to influence considerably the surface morphologies,

microstructures, crystal structures and phases, magnetic properties, complex permittivity, and permeability as well as the reflection loss in the MW frequency domain of the resultant NdBFCs. The obtained NdBFCs consisted of highly porous and roughened microstructures with a homogeneous distribution of grains. The undoped sample revealed the presence of $BaFe_{12}O_{19}$ (hexagonal lattice) and α-Fe_2O_3 (rhombohedral lattice) crystal phases. The doped specimens (NdBFC1 and NdBFC2) showed the new hexagonal crystalline phase of $Ba_3Fe_{32}O_{51}$ and $BaNd_2O_4$. The achieved minimum reflection loss with the absorption of several MW frequencies (in the range 8.2-12.4 GHz) shown by the proposed NdBFCs is established to be beneficial for the MW X-band absorber applications.

Acknowledgements

The authors are grateful to the Universitas Jenderal Soedirman, Kemenristekdikti Indonesia and UTM Malaysia (MOHE, FRGS/KPT 5F050 & UTMFR 20H65) for financial supports.

REFERENCES

[1] R. Rajesh Kanna, N. Lenin, K. Sakthipandi, M. Sivabharathy, Impact of lanthanum on structural, optical, dielectric and magnetic properties of $Mn_{1-x}Cu_xFe_{1.85}La_{0.15}O_4$ spinel nanoferrites, Ceram. Int. 43 (2017) 15868–15879. doi:10.1016/j.ceramint.2017.08.160.

[2] S.R. Bhongale, H.R. Ingawale, T.J. Shinde, P.N. Vasambekar, Effect of Nd^{3+} Substitution on Structural and Magnetic Properties of Mg-Cd Ferrites Synthesized by Microwave Sintering Technique, J. Rare Earths. 36 (2018) 390–397. doi:10.1016/j.jre.2017.11.003.

[3] M.A. Ahmed, N. Okasha, R.M. Kershi, Influence of rare-earth ions on the structure and magnetic properties of barium W-type hexaferrite, J. Magn. Magn. Mater. 320 (2008) 1146–1150. doi:10.1016/j.jmmm.2007.11.014.

[4] G. Shen, Z. Xu, Y. Li, Absorbing properties and structural design of microwave absorbers based on W-type La-doped ferrite and carbon fiber composites, J. Magn. Magn. Mater. 301 (2006) 325–330. doi:10.1016/j.jmmm.2005.07.007.

[5] W. Jing, Z. Hong, B. Shuxin, C. Ke, Z. Changrui, Microwave absorbing properties of rare-earth elements substituted W-type barium ferrite, J. Magn. Magn. Mater. 312 (2007) 310–313. doi:10.1016/j.jmmm.2006.10.612.

[6] C. Sun, K. Sun, P. Chui, Microwave absorption properties of Ce-substituted M-type barium ferrite, J. Magn. Magn. Mater. 324 (2012) 802–805. doi:10.1016/j.jmmm.2011.09.023.

[7] L. Deng, L. Ding, K. Zhou, S. Huang, Z. Hu, B. Yang, Electromagnetic properties and microwave absorption of W-type hexagonal ferrites doped with La^{3+}, J. Magn. Magn. Mater. 323 (2011) 1895–1898. doi:10.1016/j.jmmm.2011.02.034.

[8] S.S. Seyyed Afghahi, M. Jafarian, M. Salehi, Y. Atassi, Improvement of the performance of microwave X band absorbers based on pure and doped Ba-hexaferrite, J. Magn. Magn. Mater. 421 (2017) 340–348. doi:10.1016/j.jmmm.2016.08.042.

[9] W. Widanarto, F. Amirudin, S.K. Ghoshal, M. Effendi, W.T. Cahyanto, Structural and magnetic properties of La^{3+} substituted barium–natural nanoferrites as microwave absorber in X-band, J. Magn. Magn. Mater. 426 (2017) 483–486. doi:10.1016/j.jmmm.2016.11.124.

[10] Z. Qiao, S. Pan, J. Xiong, L. Cheng, Q. Yao, P. Lin, Magnetic and microwave absorption properties of La-Nd-Fe alloys, J. Magn. Magn. Mater. 423 (2017) 197–202. doi:10.1016/j.jmmm.2016.08.093.

[11] W. Widanarto, E. Ardenti, S.K. Ghoshal, C. Kurniawan, M. Effendi, W.T. Cahyanto, Significant

reduction of saturation magnetization and microwave-reflection loss in barium-natural ferrite via Nd^{3+} substitution, J. Magn. Magn. Mater. 456 (2018) 288–291. doi:10.1016/j.jmmm.2018.02.050.

[12] P. Shepherd, K.K. Mallick, R.J. Green, Magnetic and structural properties of M-type barium hexaferrite prepared by co-precipitation, J. Magn. Magn. Mater. 311 (2007) 683–692. doi:10.1016/j.jmmm.2006.08.046.

[13] M.F. Din, I. Ahmad, M. Ahmad, M.T. Farid, M. Asif Iqbal, G. Murtaza, M.N. Akhtar, I. Shakir, M.F. Warsi, M.A. Khan, Influence of Cd substitution on structural, electrical and magnetic properties of M-type barium hexaferrites co-precipitated nanomaterials, J. Alloys Compd. 584 (2014) 646–651. doi:10.1016/j.jallcom.2013.09.043.

[14] J.Y. Kwak, C.S. Lee, D. Kim, Y. Il Kim, Characteristics of Barium Hexaferrite Nanoparticles Prepared by Temperature-Controlled Chemical Coprecipitation, 56 (2012) 609–616. doi:10.5012/jkcs.2012.56.5.609.

[15] W. Li, X. Qiao, M. Li, T. Liu, H.X. Peng, La and Co substituted M-type barium ferrites processed by sol-gel combustion synthesis, Mater. Res. Bull. 48 (2013) 4449–4453. doi:10.1016/j.materresbull.2013.07.044.

[16] S.K. Chawla, R.K. Mudsainiyan, S.S. Meena, S.M. Yusuf, Sol–gel synthesis, structural and magnetic properties of nanoscale M-type barium hexaferrites $BaCo_xZr_xFe_{(12-2x)}O_{19}$, J. Magn. Magn. Mater. 350 (2014) 23–29. doi:10.1016/j.jmmm.2013.09.007.

[17] K.K. Mallick, P. Shepherd, R.J. Green, Magnetic properties of cobalt substituted M-type barium hexaferrite prepared by co-precipitation, J. Magn. Magn. Mater. 312 (2007) 418–429. doi:10.1016/j.jmmm.2006.11.130.

[18] Y. Wang, X. Gao, Y. Fu, X. Wu, Q. Wang, W. Zhang, C. Luo, Enhanced microwave absorption performances of polyaniline/graphene aerogel by covalent bonding, Compos. Part B Eng. 169 (2019) 221–228. doi:10.1016/j.compositesb.2019.04.008.

[19] Z. Gao, B. Xu, M. Ma, A. Feng, Y. Zhang, X. Liu, Z. Jia, G. Wu, Electrostatic self-assembly synthesis of $ZnFe_2O_4$ quantum dots ($ZnFe_2O_4$@C) and electromagnetic microwave absorption, Compos. Part B. 179 (2019) 107417.

[20] G. Wu, Interlayer controllable of hierarchical MWCNTs@C@FexOy cross-linked composite with wideband electromagnetic absorption performance, Compos. Part A. 128 (2020) 105687. doi:10.1016/j.compositesa.2019.105687.

[21] A. Feng, M. Ma, Z. Jia, M. Zhang, phytic acid-doped polyaniline composite and its, RSC Adv. 9 (2019) 25932–25941. doi:10.1039/c9ra04219a.

[22] Z. Gao, Z. Jia, J. Zhang, A. Feng, Z. Huang, G. Wu, Tunable microwave absorbing property of - La_xFeO_3/C by introducing A - site cation deficiency, J. Mater. Sci. Mater. Electron. 30 (2019) 13474–13487. doi:10.1007/s10854-019-01715-0.

[23] W. Widanarto, F.M. Rahayu, S.K. Ghoshal, M. Effendi, W.T. Cahyanto, Impact of ZnO substitution on magnetic response and microwave absorption capability of strontium-natural nanoferrites, Results Phys. 5 (2015) 253–256. doi:10.1016/j.rinp.2015.09.002.

[24] D. Li, K. Guo, F. Wang, Z. Wu, B. Zhong, S. Zuo, J. Tang, J. Feng, R. Zhuo, De Yan, P. Yan, Enhanced microwave absorption properties in C band of Ni/C porous nanofibers prepared by electrospinning, J. Alloys Compd. 800 (2019) 294–304. doi:10.1016/j.jallcom.2019.05.284.

[25] V.S. Vinila, R. Jacob, A. Mony, H.G. Nair, S. Issac, S. Rajan, A.S. Nair, J. Isac, XRD Studies on Nano Crystalline Ceramic Superconductor PbSrCaCuO at Different Treating Temperatures, Cryst. Struct. Theory Appl. 03 (2014) 1–9. doi:10.4236/csta.2014.31001.

[26] S. Dabagh, A.A. Ati, R.M. Rosnan, S. Zare, Z. Othaman, Effect of Cu – Al substitution on the structural and magnetic properties of Co ferrites, Mater. Sci. Semicond. Process. 33 (2015) 1–8. doi:10.1016/j.mssp.2015.01.025.

[27] W. Lixi, H. Qiang, M. Lei, Z. Qitu, Influence of Sm^{3+} Substitution on Microwave Magnetic Performance of Barium Hexaferrites, J. Rare Earths. 25 (2007) 216–219.

[28] W. Lei, L. Peihao, P. Shunkang, Z. Huaiying, Microwave absorbing properties of NdFeCo magnetic powder, J. Rare Earths. 30 (2012) 529–533. doi:10.1016/S1002-0721(12)60085-4.

[29] L. Wang, H. Yu, X. Ren, G. Xu, Magnetic and microwave absorption properties of

$BaMn_xCo_{1-x}TiFe_{10}O_{19}$, J. Alloys Compd. 588 (2014) 212–216. doi:10.1016/j.jallcom.2013.11.072.

[30] G. Wu, Y. Cheng, Z. Yang, Z. Jia, H. Wu, L. Yang, Design of carbon sphere / magnetic quantum dots with tunable phase compositions and boost dielectric loss behavior, Chem. Eng. J. 333 (2018) 519–528. doi:10.1016/j.cej.2017.09.174.

[31] C.K. Das, P. Bhattacharya, S.S. Kalra, Graphene and MWCNT: Potential Candidate for Microwave Absorbing Materials, J. Mater. Sci. Res. 1 (2012) p126. doi:10.5539/jmsr.v1n2p126.

[32] Y. Ma, Y. Zhou, Y. Sun, H. Chen, Z. Xiong, X. Li, L. Shen, Y. Liu, Tunable magnetic properties of Fe_3O_4/rGO/PANI nanocomposites for enhancing microwave absorption performance, J. Alloys Compd. 796 (2019) 120–130. doi:10.1016/j.jallcom.2019.04.310.

[33] Y. Huang, J. Ji, Y. Chen, X. Li, J. He, X. Cheng, S. He, Y. Liu, J. Liu, Broadband microwave absorption of Fe_3O_4 –$BaTiO_3$ composites enhanced by interfacial polarization and impedance matching, Compos. Part B Eng. 163 (2019) 598–605. doi:10.1016/j.compositesb.2019.01.008.

[34] K. Shi, J. Li, S. He, H. Bai, Y. Hong, Y. Wu, D. Jia, Z. Zhou, A superior microwave absorption material: Ni^{2+}-Zr^{4+} Co-Doped barium ferrite ceramics with large reflection loss and broad bandwidth, Curr. Appl. Phys. 19 (2019) 842–848. doi:10.1016/j.cap.2019.03.018.

[35] S. Salman, S.S.S. Afghahi, M. Jafarian, Y. Atassi, Microstructural and magnetic studies on $BaMg_xZn_xX_{2x}Fe_{12-4x}O_{19}$ (X=Zr,Ce,Sn) prepared via mechanical activation method to act as a microwave absorber in X-band, J. Magn. Magn. Mater. 406 (2016) 184–191. doi:10.1016/j.jmmm.2016.01.020.

[36] M.R. Meshram, N.K. Agrawal, B. Sinha, P.S. Misra, Characterization of M-type barium hexagonal ferrite-based wide band microwave absorber, J. Magn. Magn. Mater. 271 (2004) 207–214. doi:10.1016/j.jmmm.2003.09.045.

Neodymium ions activated barium ferrite composites for microwave X-band absorber applications: synthesis and characterizations

ORIGINALITY REPORT

12%	3%	11%	10%
SIMILARITY INDEX	INTERNET SOURCES	PUBLICATIONS	STUDENT PAPERS

PRIMARY SOURCES

1	Submitted to Universitas Jenderal Soedirman Student Paper	7%
2	Wahyu Widanarto, Siti Khaeriyah, Sib Krishna Ghoshal, Candra Kurniawan, Mukhtar Effendi, Wahyu Tri Cahyanto. "Selective microwave absorption in Nd3+ substituted barium ferrite composites", Journal of Rare Earths, 2019 Publication	4%
3	E Handoko, I Sugihartono, S Budi, M Randa, Z Jalil, M Alaydrus. "The effect of thickness on microwave absorbing properties of barium ferrite powder", Journal of Physics: Conference Series, 2018 Publication	1%

Exclude quotes	On	Exclude matches	< 1%
Exclude bibliography	On		